

pubs.acs.org/macroletters Letter

Coarse-Grained Artificial Intelligence for Design of Brush Networks

Andrey V. Dobrynin,* Anastasia Stroujkova, Mohammad Vatankhah-Varnosfaderani, and Sergei S. Sheiko*



Cite This: ACS Macro Lett. 2023, 12, 1510-1516



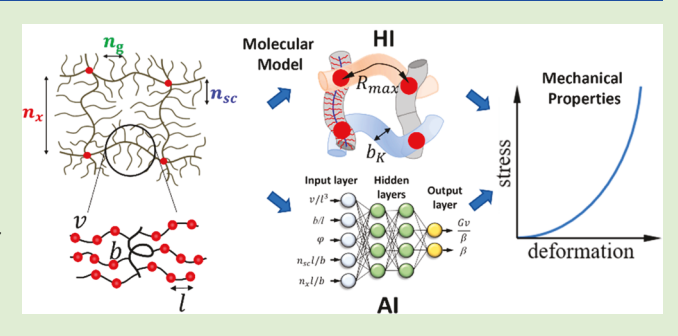
ACCESS

III Metrics & More

Article Recommendations

s Supporting Information

ABSTRACT: The ability to synthesize elastomeric materials with programmable mechanical properties is vital for advanced soft matter applications. Due to the inherent complexity of hierarchical structure—property correlations in brush-like polymer networks, the application of conventional theory-based, so-called Human Intelligence (HI) approaches becomes increasingly difficult. Herein we developed a design strategy based on synergistic combination of HI and AI tools which allows precise encoding of mechanical properties with three architectural parameters: degrees of polymerization (DP) of network strands, n_{xy} side chains, n_{sy} backbone spacers between side chains, n_{g} . Implementing a



multilayer feedforward artificial neural network (ANN), we took advantage of model-predicted structure—property cross-correlations between coarse-grained system code including chemistry specific characteristics $\mathbf{S} = [l, v, b]$ defined by monomer projection length l and excluded volume v, Kuhn length b of bare backbone and side chains, and architecture $\mathbf{A} = [n_{sc}, n_{g}, n_{x}]$ of polymer networks and their equilibrium mechanical properties $\mathbf{P} = [G, \beta]$ including the structural shear modulus G and firmness parameter G. The ANN was trained by minimizing the mean-square error with Bayesian regularization to avoid overfitting using a data set of experimental stress-deformation curves of networks with brush-like strands of poly(n-butyl acrylate), poly(isobutylene), and poly(dimethylsiloxane) having structural modulus G < 50 kPa and $0.01 \le G \le 0.3$. The trained ANN predicts network mechanical properties with 95% confidence. The developed ANN was implemented for synthesis of model networks with identical mechanical properties but different chemistries of network strands.

dvanced applications, such as soft robotics and person-Alized medicine, require elastomers with well-controlled mechanical properties. To achieve this goal, a recently developed approach implements a brush-like strand architecture to encode mechanical properties of elastomers and gels.1-12 This methodology has allowed the synthesis of networks with a wide range of softness, strain-stiffening, and extensibility, which is impossible to realize in conventional elastomers and gels made by cross-linking linear chains (Figure 1). 13-21 However, a broad practical implementation of this design-by-architecture strategy is hindered by a multiplicity of structural parameters such as degree of polymerization (DP) of the brush backbone between cross-links, n_x , side chains n_{sc} , and backbone spacer between side chains, $n_{\rm g}$. This requires further development of multivariable molecular models of networks and multiscale computer simulations, collectively called Human Intelligence (HI), for the elucidation of correlations between network molecular structure and targeted mechanical properties. 12,22-24

In contrast with HI, Artificial Intelligence (AI) based approaches allow correlating the network structure with targeted mechanical properties without the need for the development of theoretical models. The AI methodology has been successfully implemented in drug design, protein folding,

and development of materials for microelectronics.^{25–30} Extensive data mining produces Data Banks comprised of comprehensive molecular parameters, including the constituent atoms, chemical bonds, bond angles, interatomic interactions, and electronic structure. This *ab initio* approach is difficult to apply to the design of polymer networks due to their hierarchical organization spanning across length scales from monomers to network mesh size, resulting in emerging mechanical properties with no direct correlations with the chemical structure. However, hierarchical structure—property correlations open a path for the development of a coarsegrained AI approach, where the chemical specificity is encrypted in the mesoscopic structural elements such as number density, contour length, and Kuhn length of network strands introduced below.

We demonstrate the synergistic interplay of the HI and AI approaches in the design of polymer networks with targeted

Received: August 10, 2023 Revised: October 10, 2023 Accepted: October 19, 2023 Published: October 27, 2023





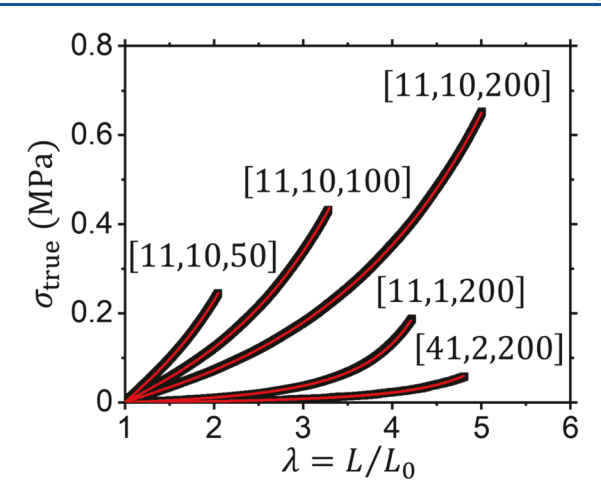


Figure 1. Examples of stress—elongation curves measured upon uniaxial extension of poly(n-butyl acrylate) (PBA) brush elastomers (thick black lines) with different architectures of network strands $[n_{sc}, n_x]$ characterized by the degree of polymerization of the brush backbone between cross-links, n_x , side chains n_{sc} and backbone spacer between side chains, n_g . Red lines show the best fit to function $\sigma_{\rm true}(\lambda)$ (eq 1), which shape is described by the structural shear modulus G and strain-stiffening parameter G. The values of the fitting parameters $[G,\beta]$ for shown data sets from left to right are [46.97 kPa, 0.108], [27.43 kPa, 0.057], [15.76 kPa, 0.031], [2.48 kPa, 0.097], and [0.65 kPa, 0.072]. For all data sets, R^2 values are better than 0.995 and errors in G and G are less than 2%.

mechanical properties, by considering one of the basic network topologies: covalently cross-linked unentangled brush-like strands (Figure 2). Their nonlinear elastic response to uniaxial extension at a constant volume is described by the following equation of state 23,32,33

$$\sigma_{\text{true}}(\lambda) = (\lambda^2 - \lambda^{-1}) \frac{G}{3} \left[1 + 2 \left(1 - \frac{\beta(\lambda^2 + 2\lambda^{-1})}{3} \right)^{-2} \right]$$
(1)

relating true stress with the sample elongation ratio $\lambda = L/L_0 \ge 1$, describing deformation from initial length, L_0 , to length, L. The shape of the stress—strain curve is defined by two parameters: the structural shear modulus, G, accounting for the

network topology and strand architecture, and the strainstiffening parameter, β , characterizing the finite extensibility of network strands manifested in divergence of stress at finite λ .

HI and AI have the same goal: predict correlations between mechanical properties $\mathbf{P}=[G,\,\beta]$ and network structure, comprised of chemistry-specific characteristics $\mathbf{S}=[l,\,\nu,\,b]$ (monomer projection length l on the end-to-end distance in all trans (zigzag) conformation and excluded volume ν (or number density $\rho=\nu^{-1}$), the Kuhn length b of the bare backbone and side chains) and network architecture $\mathbf{A}=[n_{sc},n_{g},n_{x}]$ (Figure 2). In the HI approach, different conformational regimes of brush strands are analyzed to derive analytical expressions for G and β in terms of the \mathbf{S} and \mathbf{A} descriptors. 12,23,24,31,34 This allows extrapolation of the established $\mathbf{P}(\mathbf{S},\mathbf{A})$ correlations as design rules to systems that were not previously studied. However, HI activities are time-consuming, rely on a deep understanding of polymer physics, and require recalibration of $\mathbf{P}(\mathbf{S},\mathbf{A})$ correlations each time when the chemistry of brush strands (\mathbf{S} descriptors) is changed.

In contrast, the coarse-grained AI approach does not involve any theoretical analysis of the strands' conformational states and structure—property correlations. It utilizes a multilayer feedforward artificial neural network (ANN)³⁵ to discover hidden P(S, A) correlations without any knowledge of analytical expressions for macroscopic properties G and G in terms of G and G in terms of G and G in terms of G and G in terms of G in terms of G and G in terms of G in terms of G and G in

We represent backbones of brush-like network strands as semiflexible chains with the effective Kuhn length $b_{\rm K}$ due to steric repulsion between side chains, maximum elongation length $R_{\rm max}=n_x l$ and their number density $\rho_{\rm s}=\varphi/vn_x$ that are defined by the chemical ${\bf S}=[l,v,b]$ and architectural ${\bf A}=[n_{\rm sc},n_{\rm g},n_x]$ descriptors (Figure 2). The factor $\varphi=n_{\rm g}/(n_{\rm g}+n_{\rm sc})$ describes the dilution of the stress-supporting strands by grafting side chains with DP = $n_{\rm sc}$ separated by $n_{\rm g}$ backbone repeat units (Figure 2), where $\varphi=1$ corresponds to linear

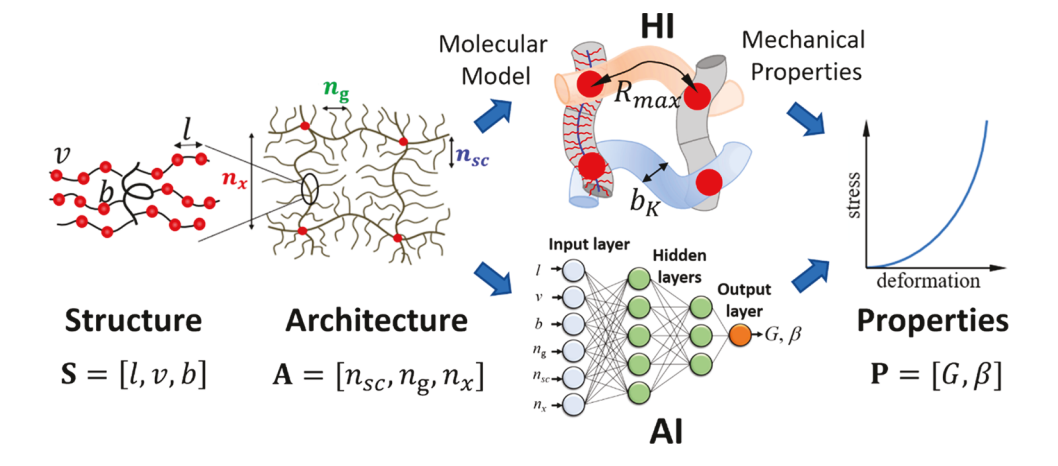


Figure 2. Workflow of HI and AI network design encoded by monomer projection length l on the end-to-end distance in all trans (zigzag) conformation, excluded volume v, and Kuhn length b of bare backbone and side chains, and network architecture $\mathbf{A} = [n_{sc}, n_g, n_x]$. The network model is defined by the length of the fully extended backbone, R_{max} , effective backbone Kuhn length due to interactions between side chains, b_{K} , and number density, ρ_s , of network strands.

chain networks with $n_{\rm sc}=0$. In this coarse-grained representation, the brush strands with the degree of polymerization of the backbone n_x between cross-links are characterized by an effective degree of polymerization (number of the effective Kuhn segments per network strand)

$$\alpha^{-1} \equiv \frac{n_x l}{b_K} = \frac{R_{\text{max}}}{b_K} \tag{2}$$

This description provides molecular interpretation of the strain-stiffening parameter as^{23,33}

$$\beta \equiv \frac{\langle R_{\rm in}^2 \rangle}{R_{\rm max}^2} = \alpha \left(1 - \frac{\alpha}{2} \left(1 - \exp\left(-\frac{2}{\alpha} \right) \right) \right) \tag{3}$$

which quantifies by how much a network strand can be stretched from its initial state with the mean-square end-to-end distance $\langle R_{\rm in}^2 \rangle$ to its fully extended state. For known β , we solve eq 3 to obtain α and thus determine the number of Kuhn segments per network strand.

For networks of semiflexible strands, the structural shear modulus is a product of the network topology coefficient (C_{top}) , number density of stress-supporting strands (ρ_s) , and their average elastic energy in a network preparation state in terms of the thermal energy $k_{\text{B}}T$,

$$G = C_{\text{top}} \rho_{\text{s}} k_{\text{B}} T \frac{\langle R_{\text{in}}^2 \rangle}{b_{\text{K}} R_{\text{max}}} = k_{\text{B}} T C_{\text{top}} \frac{\varphi}{\nu n_{x}} \beta \alpha^{-1}$$
(4)

The coefficient $C_{\rm top}$ is determined by cross-link functionality, fractions of dangling ends, and loops. The dangling ends reduce the density of stress supporting strands by n_x -dependent factor in $C_{\rm top} = C_{\rm fl}(1-n_x/N_{\rm app})$, where $N_{\rm app}$ is an apparent DP of the precursor chains and $C_{\rm fl}$ is a numerical coefficient accounting for cross-link functionality and a loop effect. This results in a relationship

$$\frac{G\alpha}{\beta\varphi} = \frac{a}{n_x} - c \tag{5}$$

reflecting partitioning of monomers between stress supporting and stress-free network strands, which was confirmed by experiments and computer simulations. 23,31,34 Numerical coefficients $a=k_{\rm B}TC_{\rm fl}/v$ and $c=k_{\rm B}TC_{\rm fl}/(vN_{\rm app})$ are determined by the selection of the polymerization scheme and specific chemistry of the network strands and are obtained by fitting experimental data. Note that n_x is typically taken from the monomer/cross-linker feed ratios, which is different from an actual DP value by a multiplicative constant.

The number of Kuhn segments per network strand, α^{-1} , is a key parameter, which defines both G and β (eqs 3 and 4) and controls the nonlinear response of the network strands (eq 1). For brush networks, the Kuhn length $b_{\rm K}$ depends on a particular conformational regime in the diagram of states (Figure 3). For combs the weak steric repulsion between loosely grafted side chains is not sufficient to stiffen brush backbone such that $b_{\rm K} \approx b$ (the bare backbone Kuhn length) and $\alpha \approx \beta$. In bottlebrushes with densely grafted side chains, $b_{\rm K}$ depends on the side chain length and grafting density. For example, in the stretched backbone (SBB) regime, we obtain

$$b_{\rm K} \cong \frac{1}{\rho l^{3/2} b^{1/2}} \frac{\varphi^{-1}}{n_{\rm sc}^{1/2} \Phi^*} \tag{6}$$

where $\Phi^* \cong 0.7$ corresponds to crossover between comb and bottlebrush regimes determined in computer simulations^{36,37}

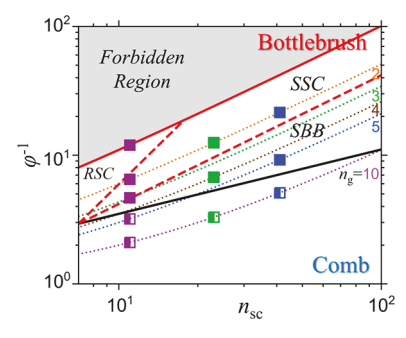


Figure 3. Diagram of states of different conformation regimes of bottlebrush and comb strands. SBB, stretched backbone subregime; SSC, stretched side chain subregime; and RSC, rod-like side chain subregime. The crossover boundaries between regimes are given by $\varphi^{-1}=\rho(bl)^{3/2}n_{\rm sc}^{1/2}\Phi^*$ (Comb/SBB), $\varphi^{-1}=\rho bl^2n_{\rm sc}\Phi^*$ (SBB/SSC), and $\varphi^{-1}=\rho^2n_{\rm sc}^2\Phi^*$ (SSC/RSC). The crossover boundaries are calculated by setting the value of the crowding parameter $\Phi^*\cong 0.7$ obtained in computer simulations. 36,37 The lower boundary (solid red) for the forbidden region $\varphi^{-1}=1+n_{\rm sc}$ was calculated with $n_{\rm g}=1$. Kuhn lengths in different regimes are given by the following equations: $b_{\rm K}\cong b({\rm Comb}),\ b_{\rm K}\cong \frac{1}{\rho^{3/2}b^{1/2}n_{\rm sc}^{1/2}\Phi^*}$ (SBB), and $b_{\rm K}\cong \frac{1}{\rho^{1/2}l^{1/2}}(\varphi^{-1}/\Phi^*)^{1/2}$ (SSC). The following set of parameters was used for diagram calculations: $\rho^{-1}=\nu=0.195~{\rm nm}^3, l=0.255~{\rm nm}, b=1.79~{\rm nm}.$

and used in construction of diagram of states (Figure 3). Thus, using eq 6 we can write down

$$\alpha = C_{\alpha}/n_{x}\varphi n_{\rm sc}^{1/2} \tag{7}$$

where C_{α} is a constant depending on the polymer specific chemistry. Equations 3, 5, and 7 provide relationships between macroscopic network properties described by $\mathbf{P} = [G, \beta]$ and brush strand chemistry $\mathbf{S} = [l, v, b]$ and architecture $\mathbf{A} = [n_{sc}, n_g, n_x]$. These equations define a line in 3D space $[n_{sc}, n_g, n_x]$, which corresponds to a particular G and G values adding flexibility in selection of strand molecular architecture. This approach was implemented to design of brush networks with programmable mechanical properties using poly(n-butyl acrylate) (PBA), poly(isobutylene) (PIB), and poly-(dimethylsiloxane) (PDMS) polymers as building blocks. 12,31,34 However, these HI-determined structure—property correlations require knowledge of the network parameters $[a, c, C_{\alpha}]$, which should be obtained each time the brush chemistry and network architecture are changed.

The established relationships between the network architecture and its deformation response indicate that, with a large enough data set, we should be able to use an AI-based approach to predict network architectures with desired properties and vice versa. For our data set of 73 brush networks of poly(n-butyl acrylate) (PBA), polyisobutylene (PIB), and poly(dimethylsiloxane) (PDMS), $^{12,31,34}_{i}$ we use a multilayer feedforward artificial neural networks (ANN) with Bayesian regularization 35 to find relationships between a set of n input variables i_j (input n-dimensional vector \mathbf{I} with components i_j) and a set of corresponding k output (target) variables t_j (output k-dimensional vector \mathbf{T} with components t_j) in the following form 35,38

$$t_j = f(\mathbf{I}) + e_j \tag{8}$$

where $f(\mathbf{I})$ is the unknown function and e_j is the Gaussian noise representing the experimental errors. ANN training involves minimization of the sum of squared residuals

$$E_R = \sum_{j=1}^{k} (t_j - est_j)^2$$
 (9)

where t_j are the known output values and est_j are the values estimated by the ANN. Minimization of the objective function in eq 9 was performed using the Levenberg–Marquardt optimization method.³⁹ To avoid overfitting in small data sets containing experimental errors, we implemented Bayesian regularization.^{35,40} This was done by adding an extra term to the objective function³⁸

$$F = \gamma E_{\rm R} + \delta E_{\rm W} \tag{10}$$

where $E_{\rm W}$ is the sum of squared ANN weights. The parameters of the objective function γ and δ are initially set to 0 and 1 respectively and then updated at each Levenberg–Marquardt step. The program for ANN-based data analysis was written in MATLAB using built-in ANN functions, Levenberg–Marquardt optimization, and Bayesian regularization.

The input layer is represented by five variables $(i_j; Figure 4a)$. In particular, we reduced the structural S = [l, v, b] and architectural $A = [n_{sc}, n_g, n_x]$ sets describing a network to a five-dimensional input vector

$$\mathbf{I} = \left[\frac{b}{l}, \frac{v}{l^3}, \varphi, \frac{n_{sc}l}{b}, \frac{n_x l}{b} \right] \tag{11}$$

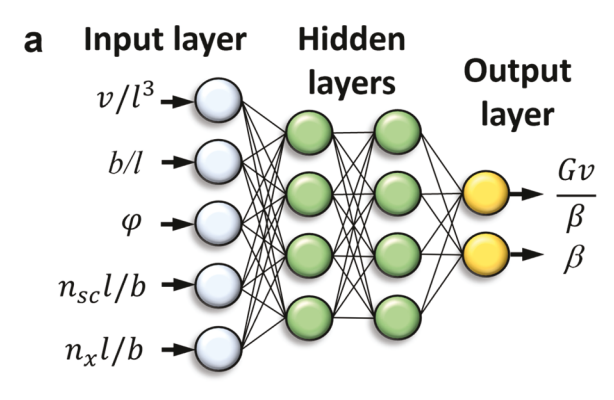
This selection of the input vector components is rationalized by the fact that the polymer properties are characterized by chain rigidity described by the number of Kuhn segments per side chain and brush backbone rather than their chemical DPs $[n_{sv}, n_{sc}]$. Furthermore, brush diagram of states is a universal function of φ , where boundaries between different regimes (Figure 3) and corresponding effective Kuhn lengths of brush strands renormalized by repulsion between side chains (eq 6) are expressed in terms of b/l and v/l^3 , brush composition φ , and the number of Kuhn segments per side chain $n_{sc}l/b^{36}$ using chemistry specific set of S = [l, v, b].

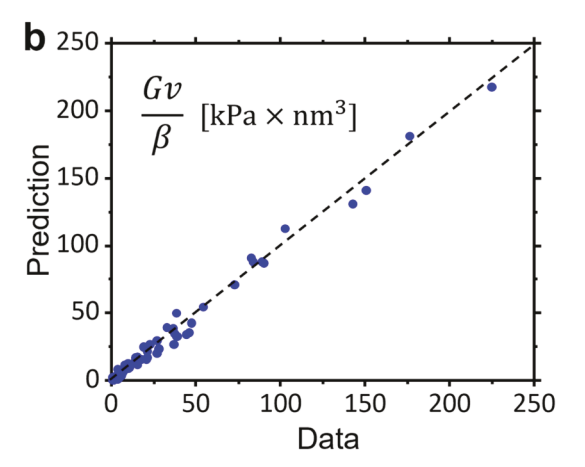
The input layer is followed by two hidden layers consisting of four neurons each (Figure 4a). The number of neurons in the hidden layers was determined by using preliminary trial and error tests to provide the desired performance without overfitting. For example, an increase in the number of hidden layers resulted in data overfitting with improved performance on the training set but poor generalization performance. Each neuron in the hidden layers performs a weighted summation of the inputs prior to activation, which is then passed to a nonlinear activation function.

The two-dimensional output vector describing mechanical properties of the network has components

$$\mathbf{T} = \left[\frac{G\nu}{\beta}, \beta \right] \tag{12}$$

We use Gv/β to eliminate the dependence of G on β and monomer packing density (eq 4). This allows us to directly correlate the mechanical properties with the strand rigidity and network architecture. It is also possible to normalize the structural modulus by k_BT thus using a monomer-type specific modulus, $G_m = k_BT/\nu$, as a normalization factor. However, this





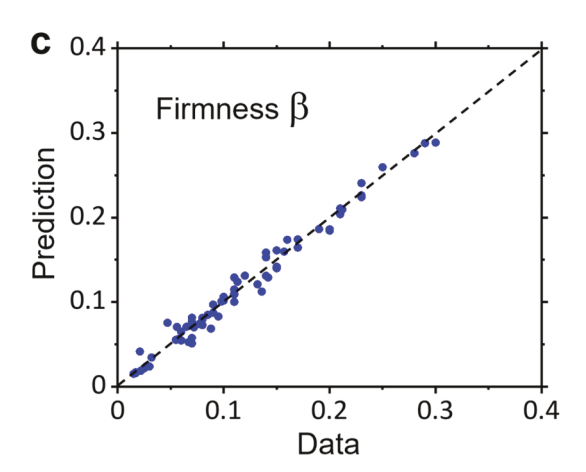


Figure 4. (a) Schematic representation of the neural network used for brush networks. Results of the ANN for (b) normalized structural modulus Gv/β and (c) firmness parameter β . The following sets of structural parameters are used in calculations: PBA ($v = 0.195 \text{ nm}^3$, l = 0.255 nm, b = 1.79 nm); PIB ($v = 0.111 \text{ nm}^3$, l = 0.255 nm, b = 1.2 nm); PDMS ($v = 0.127 \text{ nm}^3$, l = 0.3 nm, b = 1.13 nm).

is not necessary since measurements are conducted at a fixed (e.g., room) temperature.

A data set is composed of I and T vectors of brush-like networks with systematically varied S and A descriptors along with the corresponding G and β measured experimentally. Before network training runs, the data set is randomly divided into three subsets: the training subset, the validation subset, and the test subset. The training set is used for computing the network weights and biases by the minimization of the objective function. The validation subset is used for monitoring error during the training process. Normally both

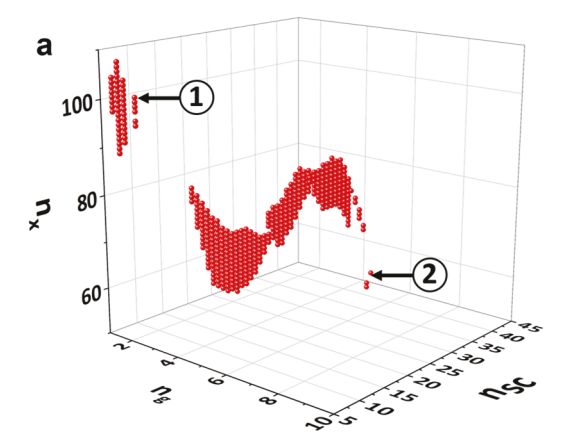
training and validation errors decrease at the beginning of the network training. However, at the later stages, the error for the validation set may start rising, even though the error for the training set continues to decrease (network overfitting). To avoid overfitting, a training run stops when the minimum error is reached for the validation set. The test subset is excluded from the network training and validation data sets. Instead, it is used to calculate the error after the training is complete to determine the network generalization capability. The percentage of the training, validation, and testing data is 80%, 10%, and 10%, respectively.

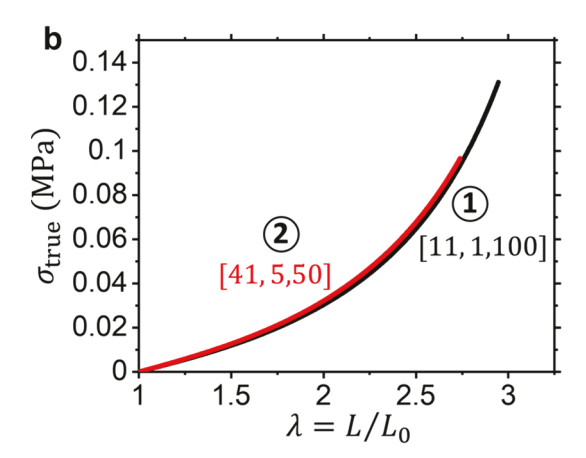
Each time a neural network is trained, the output obtained from each run can result in a different solution mainly due to (a) different initial weights and bias values and (b) different ways of data splitting into training, validation, and test sets (or into training and testing). As a result, function approximation using the same neural network architectures trained on the same data set can produce different outputs for the same input because it converges to different local minima. To avoid local minima convergence and eliminate spurious effects caused by random starting values, we trained multiple ANNs. In total, we performed two sets of 400 simulation runs of random partitioning of the data between training, validation and verification data sets. For the best network, we achieved >95% accuracy in correlation between measured and predicted values of T vector components (Figure 4b,c). It appears that the ANN provides a better prediction of the strain-stiffening parameter β compared to G.

Finally, to test ANN we predict different network structures with the nearly same stress-elongation curves but synthesized with either different monomers or different architectures, i.e., different S and A descriptors, respectively. For obtaining specific values of input vector I (eq 11), corresponding to $G \cong$ 5.9 ± 0.2 kPa and $\beta \approx 0.15 \pm 0.01$, we performed a grid search in a 3D space described by $[n_{sc}, n_{g}, n_{x}]$ (Figure 5a). The 3D map (plot) provides different sets of $[n_{sc}, n_g, n_x]$ for PBA networks with the G and β within $\pm 5\%$ from the desired value. To validate these predictions, we synthesized PBA networks (Supporting Information) with different $[n_{sc}, n_{g}, n_{x}]$ combinations yet very similar deformation responses (Figure 5b). Such maps can be created for any given chemical composition and targeted mechanical properties. By sensibly adjusting $[n_{sc}, n_{g}]$ n_x], we also synthesized brush networks with PIB, PBA and PDMS side chains (Supporting Information) that show nearly identical stress-strain curves (Figure 5c).

We illustrated synergistic implementation of the HI- and AI-based designs of brush-like networks with programmable mechanical properties. The HI approach relies on an in-depth analysis of conformational regimes and network topologies (Figure 3), and synthesis of the network library to obtain numerical coefficients connecting S, A sets with network mechanical characteristics described by G and β (eqs 3, 5, and 7). HI allows extrapolation of the network design rules outside of the explored chemistries and architectures even for small data sets. However, the application of HI tools becomes increasingly limited for complex network architectures with hierarchically organized structure—property correlations.

Conventional AI approaches to materials design, while bypassing theoretical analysis, usually require large data sets, including atomic and molecular details. This complicates the design process to achieve the required predictive power. Here we showed that judicious selection of the input parameters and implementation of the ANN with Bayesian regularization, one





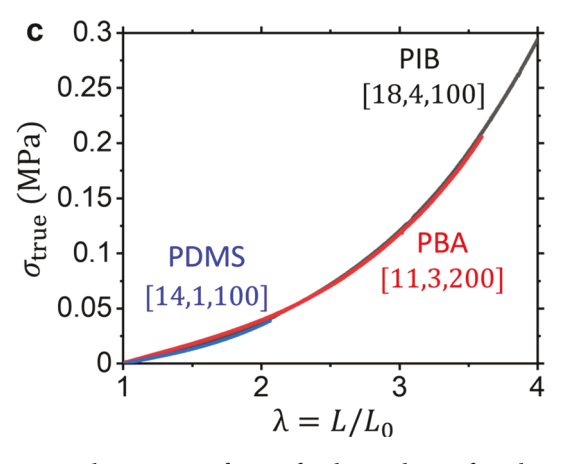


Figure 5. Implementation of ANN for the synthesis of mechanically similar networks with different chemistries and architectures. (a) Possible $[n_{sc}, n_g, n_x]$ combinations of PBA elastomers ($v=0.195 \text{ nm}^3$, l=0.255 nm, b=1.79 nm) with $G\cong 5.9\pm 0.2 \text{ kPa}$ and $\beta\cong 0.15\pm 0.01$. Numbers 1 and 2 correspond to the samples in (b). (b) Nearly identical stress—elongation curves with $G\cong 6.0 \text{ kPa}$ and $\beta\cong 0.15 \text{ of}$ two PBA elastomers with different $[n_{sc}, n_g, n_x]$ codes as indicated and (c) Architectural codes $[n_{sc}, n_g, n_x]$ of chemically dissimilar (PIB, PBA, and PDMS) brush elastomers were adjusted to show nearly identical deformation responses characterized by $G\cong 10 \text{ kPa}$ and $\beta\cong 0.07$.

could use a relatively small data set of 73 networks to achieve a successful design of network architectures with programmed mechanical properties (Figure 5b,c). The unique ANN capability of predicting different network structures with

similar mechanical properties provides multiple choices for polymer synthesis as well as product optimization in terms of safety, application limitations, and stability. The impact of AI becomes even more evident in the design of brush-like networks with mixed side chains⁴³ and brush copolymer networks,^{6,11,44–46} in which the number of the structural parameters increases exponentially to be analyzed by HI tools in the entire parameter space. Implementation of a recently developed network forensic approach to network analysis⁴⁷ should allow for a better selection and quality verification of the input data for AI training.

ASSOCIATED CONTENT

Supporting Information

The Supporting Information is available free of charge at https://pubs.acs.org/doi/10.1021/acsmacrolett.3c00479.

Synthesis description, characterization, and mechanical testing (PDF)

AUTHOR INFORMATION

Corresponding Authors

Andrey V. Dobrynin — Department of Chemistry, University of North Carolina at Chapel Hill, Chapel Hill, North Carolina 27599, United States; ⊚ orcid.org/0000-0002-6484-7409; Email: avd@email.unc.edu

Sergei S. Sheiko — Department of Chemistry, University of North Carolina at Chapel Hill, Chapel Hill, North Carolina 27599, United States; Orcid.org/0000-0003-3672-1611; Email: sergei@email.unc.edu

Authors

Anastasia Stroujkova — Department of Earth, Marine and Environmental Sciences, University of North Carolina at Chapel Hill, Chapel Hill, North Carolina 27559, United States; © orcid.org/0000-0003-3196-0170

Mohammad Vatankhah-Varnosfaderani — Department of Chemistry, University of North Carolina at Chapel Hill, Chapel Hill, North Carolina 27599, United States;
ocid.org/0000-0001-7636-9099

Complete contact information is available at: https://pubs.acs.org/10.1021/acsmacrolett.3c00479

Author Contributions

CRediT: Andrey V. Dobrynin conceptualization, methodology, supervision; Anastasia Stroujkova methodology, software, writing-review & editing; Mohammad Vatankhah-Varnosfaderani investigation, methodology, writing-review & editing; Sergei S Sheiko conceptualization, methodology, supervision, writing-review & editing.

Notes

The authors declare no competing financial interest.

ACKNOWLEDGMENTS

This work was supported by the National Science Foundation under Grants DMR 1921835, DMR 1921923, DMR 2049518, DMR 2324167, and DMR 2004048.

REFERENCES

(1) Neugebauer, D.; Zhang, Y.; Pakula, T.; Sheiko, S. S.; Matyjaszewski, K. Densely-Grafted and Double-Grafted PEO Brushes via ATRP. A Route to Soft Elastomers. *Macromolecules* **2003**, *36*, 6746–6755.

- (2) Jha, S.; Dutta, S.; Bowden, N. B. Synthesis of Ultralarge Molecular Weight Bottlebrush Polymers Using Grubbs' Catalysts. *Macromolecules* **2004**, *37*, 4365–4374.
- (3) Pakula, T.; Zhang, Y.; Matyjaszewski, K.; Lee, H. I.; Boerner, H.; Qin, S. H.; Berry, G. C. Molecular Brushes as Super-Soft Elastomers. *Polymer* **2006**, *47*, 7198–7206.
- (4) Lee, H.-i.; Pietrasik, J.; Sheiko, S. S.; Matyjaszewski, K. Stimuli-Responsive Molecular Brushes. *Prog. Polym. Sci.* **2010**, *35*, 24–44.
- (5) Feng, C.; Li, Y.; Yang, D.; Hu, J.; Zhang, X.; Huang, X. Well-Defined Graft Copolymers: from Controlled Synthesis to Multipurpose Applications. *Chem. Soc. Rev.* **2011**, *40*, 1282–1295.
- (6) Rzayev, J. Molecular Bottlebrushes: New Opportunities in Nanomaterials Fabrication. ACS Macro Lett. 2012, 1, 1146–1149.
- (7) Daniel, W. F. M.; Burdynska, J.; Vatankhah-Varnoosfaderani, M.; Matyjaszewski, K.; Paturej, J.; Rubinstein, M.; Dobrynin, A. V.; Sheiko, S. S. Solvent-Free, Supersoft and Superelastic Bottlebrush Melts and Networks. *Nat. Mater.* **2016**, *15*, 183–189.
- (8) Zhang, J.; Schneiderman, D. K.; Li, T.; Hillmyer, M. A.; Bates, F. S. Design of Graft Block Polymer Thermoplastics. *Macromolecules* **2016**, 49, 9108–9118.
- (9) Bolton, J.; Rzayev, J. Synthesis and Melt Self-Assembly of PS-PMMA-PLA Triblock Bottlebrush Copolymers. *Macromolecules* **2014**, 47, 2864–2874.
- (10) Daniel, W. F. M.; Xie, G.; Vatankhah-Varnoosfaderani, M.; Burdyńska, J.; Li, Q.; Nykypanchuk, D.; Gang, O.; Matyjaszewski, K.; Sheiko, S. S. Bottlebrush-Guided Polymer Crystallization Resulting in Supersoft and Reversibly Moldable Physical Networks. *Macromolecules* **2017**, *50*, 2103–2111.
- (11) Verduzco, R.; Li, X. Y.; Pesek, S. L.; Stein, G. E. Structure, Function, Self-Assembly, and Applications of Bottlebrush Copolymers. *Chem. Soc. Rev.* **2015**, *44*, 2405–2420.
- (12) Maw, M.; Morgan, B. J.; Dashtimoghadam, E.; Tian, Y.; Bersenev, E. A.; Maryasevskaya, A. V.; Ivanov, D. A.; Matyjaszewski, K.; Dobrynin, A. V.; Sheiko, S. S. Brush Architecture and Network Elasticity: Path to the Design of Mechanically Diverse Elastomers. *Macromolecules* **2022**, *55*, 2940–2951.
- (13) Wichterle, O.; Lim, D. Hydrophilic gels for biological use. *Nature* **1960**, *185*, 117–118.
- (14) Williams, D. F. On the mechanisms of biocompatibility. *Biomaterials* **2008**, 29, 2941–2953.
- (15) Chen, Q. Z.; Liang, S. L.; Thouas, G. A. Elastomeric biomaterials for tissue engineering. *Prog. Polym. Sci.* **2013**, 38, 584–671
- (16) Green, J. J.; Elisseeff, J. H. Mimicking biological functionality with polymers for biomedical applications. *Nature* **2016**, *540*, 386–394.
- (17) Griffith, L. G.; Naughton, G. Tissue Engineering Current Challenges and Expanding Opportunities. *Science* **2002**, *295*, 1009–1014.
- (18) Lv, S.; Dudek, D. M.; Cao, Y.; Balamurali, M. M.; Gosline, J.; Li, H. B. Designed biomaterials to mimic the mechanical properties of muscles. *Nature* **2010**, *465*, 69–73.
- (19) Storm, C.; Pastore, J. J.; MacKintosh, F. C.; Lubensky, T. C.; Janmey, P. A. Nonlinear Elasticity in Biological Gels. *Nature* **2005**, 435, 191–194.
- (20) Sun, J. Y.; Zhao, X. H.; Illeperuma, W. R. K.; Chaudhuri, O.; Oh, K. H.; Mooney, D. J.; Vlassak, J. J.; Suo, Z. G. Highly stretchable and tough hydrogels. *Nature* **2012**, *489*, 133–136.
- (21) Yu, B.; Kang, S. Y.; Akthakul, A.; Ramadurai, N.; Pilkenton, M.; Patel, A.; Nashat, A.; Anderson, D. G.; Sakamoto, F. H.; Gilchrest, B. A.; Anderson, R. R.; Langer, R. An elastic second skin. *Nat. Mater.* **2016**, *15*, 911–918.
- (22) Cao, Z.; Carrillo, J.-M. Y.; Sheiko, S. S.; Dobrynin, A. V. Computer Simulations of Bottle Brushes: From Melts to Soft Networks. *Macromolecules* **2015**. *48*. 5006–5015.
- (23) Liang, H.; Sheiko, S. S.; Dobrynin, A. V. Supersoft and Hyperelastic Polymer Networks with Brushlike Strands. *Macromolecules* **2018**, *51*, 638–645.

- (24) Sheiko, S. S.; Dobrynin, A. V. Architectural code for rubber elasticity: From supersoft to superfirm materials. *Macromolecules* **2019**, *52*, 7531–7546.
- (25) Gubernatis, J. E.; Lookman, T. Machine learning in materials design and discovery: Examples from the present and suggestions for the future. *Phys. Rev. Matt.* **2018**, *2*, 120301–1–15.
- (26) Raccuglia, P.; Elbert, K. C.; Adler, P. D. F.; Falk, C.; Wenny, M. B.; Mollo, A.; Zeller, M.; Friedler, S. A.; Schrier, J.; Norquist, A. J. Machine-learning-assisted materials discovery using failed experiments. *Nature* **2016**, *533*, 73–77.
- (27) Ceriotti, M. Unsupervised machine learning in atomistic simulations, between predictions and understanding. *J. Chem. Phys.* **2019**, *150*, 150901–1–10.
- (28) Himanen, L.; Geurts, A.; Foster, A. S.; Rinke, P. Data-Driven Materials Science: Status, Challenges, and Perspectives. *Adv. Sci.* **2019**, *6*, 1900808.
- (29) Mater, A. C.; Coote, M. L. Deep learning in chemistry. *J. Chem. Inf. Model.* **2019**, *59*, 2545–2559.
- (30) Webb, M. A.; Jackson, N. E.; Gil, P. S.; de Pablo, J. J. Targeted sequence design within the coarse-grained polymer genome. *Sci. Adv.* **2020**, *6*, No. eabc6216.
- (31) Vatankhah-Varnosfaderani, M.; Daniel, W. F. M.; Everhart, M. H.; Pandya, A. A.; Liang, H.; Matyjaszewski, K.; Dobrynin, A. V.; Sheiko, S. S. Mimicking Biological Stress-Strain Behavior with Synthetic Elastomers. *Nature* **2017**, *549*, 497–501.
- (32) Dobrynin, A. V.; Carrillo, J.-M. Y. Universality in Nonlinear Elasticity of Biological and Polymeric Networks and Gels. *Macromolecules* **2011**, *44*, 140–146.
- (33) Carrillo, J.-M. Y.; MacKintosh, F. C.; Dobrynin, A. V. Nonlinear Elasticity: From Single Chain to Networks and Gels. *Macromolecules* **2013**, *46*, 3679–3692.
- (34) Vatankhah-Varnoosfaderani, M.; Daniel, W. F. M.; Zhushma, A. P.; Li, Q.; Morgan, B. J.; Matyjaszewski, K.; Armstrong, D. P.; Spontak, R. J.; Dobrynin, A. V.; Sheiko, S. S. Bottlebrush Elastomers: A New Platform for Freestanding Electroactuation. *Adv. Mater.* **2017**, 29, No. 1604209.
- (35) MacKay, D. J. C. A Practical Bayesian Framework for Backpropagation Networks. *Neural Computation* **1992**, *4*, 448–472.
- (36) Liang, H.; Cao, Z.; Wang, Z.; Sheiko, S. S.; Dobrynin, A. V. Combs and Bottlebrushes in a Melt. *Macromolecules* **2017**, *50*, 3430–3437.
- (37) Liang, H.; Wang, Z.; Sheiko, S. S.; Dobrynin, A. V. Comb and Bottlebrush Graft Copolymers in a Melt. *Macromolecules* **2019**, *52*, 3942–3950.
- (38) Foresee, F. D.; Hagan, M. T. Gauss-Newton approximation to Bayesian Learning. *Proceedings of the International Joint Conference on Neural Networks* **1997**, *3*, 1930–1935.
- (39) Hagan, M. T.; Menhaj, M. Training multilayer networks with the Marquardt algorithm. *IEEE Transactions on Neural Networks* **1994**, 5, 989–993.
- (40) Okut, H., Bayesian Regularized Neural Networks for Small n Big p Data. In *Artificial Neural Networks. Models and Applications*, Rosa, J. L. G., Ed. InTech: Rijeka, Croatia, 2016; pp 27–48.
- (41) Rubinstein, M.; Colby, R. H. *Polymer Physics*. Oxford University Press: New York, 2003.
- (42) Mark, J. E. Physical Properties of Polymers Handbook. 2nd ed.; Springer: New York, NY, 2007.
- (43) Keith, A. N.; Clair, C.; Lallam, A.; Bersenev, E. A.; Ivanov, D. A.; Tian, Y.; Dobrynin, A. V.; Sheiko, S. S. Independently Tuning Elastomer Softness and Firmness by Incorporating Side Chain Mixtures into Bottlebrush Network Strands. *Macromolecules* **2020**, *53*, 9306–9312.
- (44) Bates, C. M.; Chang, A. B.; Momcilovic, N.; Jones, S. C.; Grubbs, R. H. ABA Triblock Brush Polymers: Synthesis, Self-Assembly, Conductivity, and Rheological Properties. *Macromolecules* **2015**, *48*, 4967–4973.
- (45) Zhang, J.; Li, T.; Mannion, A. M.; Schneiderman, D. K.; Hillmyer, M. A.; Bates, F. S. Tough and Sustainable Graft Block Copolymer Thermoplastics. *ACS Macro Lett.* **2016**, *5*, 407–412.

- (46) Vatankhah-Varnosfaderani, M.; Keith, A. N.; Cong, Y. D.; Liang, H. Y.; Rosenthal, M.; Sztucki, M.; Clair, C.; Magonov, S.; Ivanov, D. A.; Dobrynin, A. V.; Sheiko, S. S. Chameleon-like elastomers with molecularly encoded strain-adaptive stiffening and coloration. *Science* **2018**, *359*, 1509–1513.
- (47) Dobrynin, A. V.; Tian, Y.; Jacobs, M.; Nikitina, E. A.; Ivanov, D. A.; Maw, M.; Vashahi, F.; Sheiko, S. S. Forensics of Polymer Networks. *Nat. Mater.* **2023**, *22*, na.